

Gaussian Mixture Measurements for Very Long Range Tracking

Qian Zhang, Taek Lyul Song

Department of Electronic Systems Engineering, Hanyang University, Hanyang, Republic of Korea

Keywords: Nonlinear Estimation, Very Long Range Tracking, Gaussian Mixtures, GMM-ITS.

Abstract: Target tracking with very long range is studied in this paper. Such tracking problem has severe measurement nonlinearity that will cause consistency problems and large tracking errors. Gaussian mixture measurements are obtained by dividing the measurement likelihood into several Gaussian components. The Gaussian Mixture Measurement-Integrated Track Splitting (GMM-ITS) is applied to very long range tracking scenarios. The simulation results show that the GMM-ITS can produce consistency in the filtering results crucial to the filter performance. Furthermore, it is also able to estimate the target state accurately with small tracking errors.

1 INTRODUCTION

Phased array radar can produce measurements which are very accurate in the range direction and very inaccurate in the cross range direction. Very long range tracking with phased array radar is an interesting but challenging problem. Due to the thin, curved, contact lens-like shape of the measurement uncertainty region in the Cartesian coordinates, this problem is also known as the contact lens problem (Tian and Bar-Shalom, 2009). The contact lens problem results in severe measurement nonlinearity that leads to corresponding consistency problems for traditional nonlinear filtering techniques such as the extended Kalman filter (EKF) (Bar-Shalom et al., 2001), the unscented Kalman filter (UKF) (Julier and Uhlmann, 2004) and the particle filter (PF) (Ristic et al., 2004). When estimating the state of a dynamic system, a state estimator is called consistent if the estimation errors based on a finite number of samples (measurements) are consistent with their theoretical statistical properties: (a) have mean zero; (b) have covariance matrix as calculated by the filter (Bar-Shalom et al., 2001).

The converted measurement Kalman filter (CMKF) (Bar-Shalom et al., 2001) transforms the polar measurement to Cartesian coordinates and implements the Kalman filter purely in the Cartesian coordinates. As the converted measurements always use a decreased accuracy in the range direction, the CMKF can produce consistent filtering results. However, measurement transformation will result in the CMKF with significant loss in range accuracy. To reduce the corresponding loss in range accuracy, the

measurement covariance adaptive extended Kalman filter (MCAEKF) employing the measurement covariance adaptive (MCA) rule was proposed in (Tian and Bar-Shalom, 2009) to address the contact lens problem. The MCA rule guarantees the consistency of the linearized EKF by artificially increasing the measurement uncertainty region. If the MCA rule is not satisfied, the standard deviation of the range measurement is increased in the MCAEKF. By modifying the covariance matrix of the measurements, the MCAEKF can yield consistent filtering results and avoid overall loss in range accuracy. The MCAEKF also has advantages in tracking accuracy. Unfortunately, it causes significant loss in accuracy at the early stage of filtering due to the artificially enlarged range measurement covariance. In order to prevent this loss, consistency-based Gaussian mixture filtering (CbGMF) (Tian and Bar-Shalom, 2014) approximates the inaccurate track using a set of sub-tracks so that the MCA rule is satisfied at the sub-track level. In the CbGMF, if there is at least one sub-track that covers the true target state, the consistency of the whole set of sub-tracks is guaranteed. To control complexity, the CbGMF removes sub-tracks that are far away from the true target state and sets an upper limit for the total number of sub-tracks. Simulation results of (Tian and Bar-Shalom, 2014) indicate that CbGMF overcomes the loss in accuracy, but still results in a small degradation in consistency.

The original and partial version of the Gaussian Mixture Measurement-Integrated Track Splitting (GMM-ITS) is proposed in (Mušicki and Evans, 2006). In this paper, we solve the contact lens prob-

lem using the GMM-ITS. The key idea of the GMM-ITS is that both the non-linear (non-Gaussian) target measurement likelihood and the target state probability density function (pdf) are approximated by a Gaussian mixture of components (Mušicki, 2009). For very long range target tracking, the GMM-ITS should divide a curved (contact lens-shaped) uncertainty measurement region (non-Gaussian) into several components. Then, each predicted track component uses each measurement component to obtain a new track component. Finally, the track component pruning and merging are performed to control the complexity of the algorithm.

The remainder of the paper is structured as follows. The details about the contact lens problem are presented in Section 2. Section 3 describes the GMM-ITS solution. A simulation study in Section 4 shows the effectiveness of this solution, followed by the conclusions.

2 PROBLEM STATEMENT

In this paper, we consider a two-dimensional measurement situation with range and azimuth. The target follows the continuous white noise acceleration (CWNA) motion model (Bar-Shalom et al., 2001) and the state vector components are ordered as

$$x = [x, y, \dot{x}, \dot{y}]' \quad (1)$$

The dynamic model is given by

$$x_k = Fx_{k-1} + v_{k-1} \quad (2)$$

where the state propagation matrix

$$F = \begin{bmatrix} 1 & T \\ 0 & 1 \end{bmatrix} \otimes I_2 \quad (3)$$

does not change with time, v_{k-1} is a sequence of zero mean, white Gaussian noise with covariance

$$Q_{k-1} = \begin{bmatrix} T^3/3 & T^2/2 \\ T^2/2 & T \end{bmatrix} \otimes \text{diag}(q_x, q_y) \quad (4)$$

T is the sampling time, I_2 is 2×2 identity matrix, q_x and q_y are power spectral densities.

The measurements are taken in polar coordinates and given by

$$b_k = h(x_k) + \omega_k \quad (5)$$

where

$$h(x_k) = \begin{bmatrix} r_k \\ \theta_k \end{bmatrix} = \begin{bmatrix} \sqrt{x_k^2 + y_k^2} \\ \tan^{-1} \left(\frac{y_k}{x_k} \right) \end{bmatrix} \quad (6)$$

$$\omega_k = \begin{bmatrix} \omega_k^r \\ \omega_k^\theta \end{bmatrix} \quad (7)$$

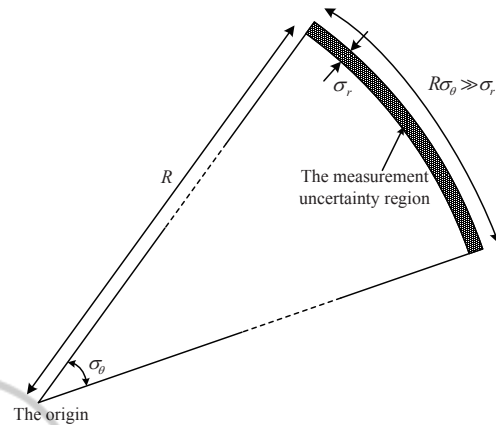


Figure 1: An example of the curved measurement uncertainty region

The measurement noise ω_k^r and ω_k^θ are assumed to be mutually independent white Gaussian with zero means and standard deviations σ_r and σ_θ , respectively. We also use B^k to denote the set of all measurements up to time k

$$B^k = \{b_k, B^{k-1}\} = \{b_k, b_{k-1}, \dots, b_1\}. \quad (8)$$

In this paper, the raw measurements (range and angle) in the polar coordinates are converted to pseudo measurements in the Cartesian coordinates. The converted measurements can be expressed as

$$z_k = Hx_k + \bar{\omega}_k \quad (9)$$

where the converted measurement noise $\bar{\omega}_k = [\omega_k^x, \omega_k^y]'$ is non-Gaussian state-dependent and ω_k^x and ω_k^y are correlated. The measurement matrix H is

$$H = [I_2 \quad 0_2] \quad (10)$$

where 0_2 is 2×2 zeros matrix. In the same way, Z^k denotes the set of all measurements up to time k

$$Z^k = \{z_k, Z^{k-1}\} = \{z_k, z_{k-1}, \dots, z_1\}. \quad (11)$$

For very long range tracking scenarios, the contact lens problem appears when the target states in the Cartesian coordinates are updated with nonlinear measurements from a different coordinate system (e.g., the polar coordinates). As the range measurement is very accurate compared to the angle measurement for very long range target tracking, the measurement uncertainty has a very thin, curved, contact lens-like shape in the Cartesian coordinates. An example of the uncertainty region of such a measurement is presented in Figure 1. We can determine from the basic geometry that the cross-range uncertainty increases while the range becomes larger. Since the accuracy in range does not change, the measurement

uncertainty region takes on an increasingly curved shape as the range increases. If the measurement non-linearity becomes too severe, the conventional filters (e.g., the EKF, the UKF and the PF) develop a significant consistency problem. In order to prevent this problem, the CMKF always reduces the accuracy in range and the MCAEKF artificially modifies the measurement covariance at the early stages of the filtering. Besides, the CbGMF approximates an inaccurate track by a set of sub-tracks.

3 THE GMM-ITS SOLUTION

In the GMM-ITS, the *a posteriori* target state estimate pdf is updated by the Bayes formula, given by

$$p(x_k|Z^k) = \frac{p(z_k|x_k)p(x_k|Z^{k-1})}{p(z_k|Z^{k-1})} \quad (12)$$

where $p(z_k|x_k)$ is the likelihood of the measurement z_k , $p(x_k|Z^{k-1})$ denotes the propagated state pdf from time $k-1$ to k and the prior likelihood of measurement is

$$p(z_k|Z^{k-1}) = \int_{x_k} p(z_k|x_k)p(x_k|Z^{k-1})dx_k. \quad (13)$$

Then, the equation (12) can be expressed as

$$p(x_k|Z^k) = \frac{p(z_k|x_k)p(x_k|Z^{k-1})}{\int_{x_k} p(z_k|x_k)p(x_k|Z^{k-1})dx_k}. \quad (14)$$

As the likelihood function of the converted measurement $p(z_k|x_k)$ is not Gaussian, the GMM-ITS seeks to approximate both $p(z_k|x_k)$ and $p(x_k|Z^{k-1})$ by Gaussian mixtures.

3.1 GMM Likelihood Approximation

In order to approximate $p(z_k|x_k)$ using a Gaussian mixture, we first divide the measurement uncertainty into several segments.

Suppose at time k , the measurements are r_k and θ_k with standard deviations σ_r and σ_θ , respectively. If we divide the measurement uncertainty into N segment, the angle of each segment is

$$\theta_{k,i} = \theta_k - \alpha\sigma_\theta + \left(i - \frac{1}{2}\right) \cdot \frac{2 \times \alpha\sigma_\theta}{N}, i = 1, \dots, N \quad (15)$$

with standard deviations

$$\sigma_{r,i} = \frac{1}{2} \cdot \frac{2 \times \alpha\sigma_r}{N} \quad (16)$$

where α is the constant number selected to provide sufficient coverage.

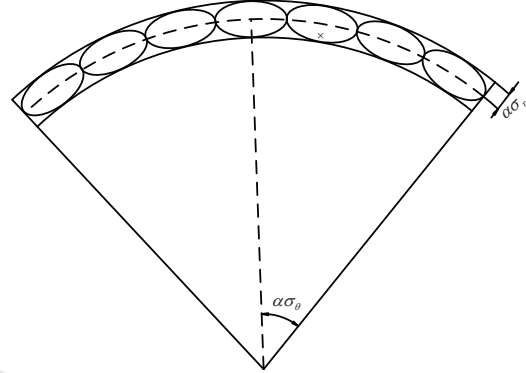


Figure 2: An example of Gaussian mixture measurement

The range of each segment is the same, given by

$$r_{k,i} = r_k, i = 1, \dots, N \quad (17)$$

with standard deviations

$$\sigma_{r,i} = \alpha\sigma_r \quad (18)$$

Each segment i is approximated by a Gaussian whose mean value and covariance are $z_{k,i}$ and $R_{k,i}$ respectively:

$$z_{k,i} = r_{k,i} \begin{bmatrix} \cos(\theta_{k,i}) \\ \sin(\theta_{k,i}) \end{bmatrix} \quad (19)$$

$$R_{k,i} = T_{k,i} \begin{bmatrix} \sigma_{r,i}^2 & 0 \\ 0 & (r_{k,i}\sigma_{\theta,i})^2 \end{bmatrix} T_{k,i}^T \quad (20)$$

with the rotation matrix $T_{k,i}$ defined by

$$T_{k,i} = \begin{bmatrix} \cos(\theta_{k,i}) & -\sin(\theta_{k,i}) \\ \sin(\theta_{k,i}) & \cos(\theta_{k,i}) \end{bmatrix} \quad (21)$$

To reflect the probability mass of the segment, a weight is associated with each segment, which satisfies

$$\lambda_{k,i} \propto \exp\left\{-\frac{(\theta_{k,i} - \theta_k)^2}{2\sigma_\theta^2}\right\} \quad (22)$$

$$\sum_{i=1}^N \lambda_{k,i} = 1 \quad (23)$$

Then, the function $p(z_k|x_k)$ is approximated by

$$p(z_k|x_k) = \sum_{i=1}^N \lambda_{k,i} \mathcal{N}(z_{k,i}; Hx_k, R_{k,i}) \quad (24)$$

where N denotes the number of measurement components and $\mathcal{N}(x; m, P)$ is the Gaussian pdf of variable x with mean m and covariance P . In equation (24), each element of the Gaussian mixture is termed a ‘‘measurement component’’. Figure 2 shows an example of the Gaussian mixture measurement model, which contains seven components. For the contact lens problem, each measurement component is presented by an α -sigma ellipse and the area of each ellipse is the same. Besides, the target is displayed by the cross.

3.2 GMM-ITS Target Tracking

In this subsection, we consider one update cycle starting with the *a posteriori* state estimate at time $k-1$, and ending with a *a posteriori* state estimate at time k . At time $k-1$, the target state pdf is approximated by a Gaussian mixture

$$p(x_{k-1}|Z^{k-1}) = \sum_{c=1}^{C_{k-1}} \xi_{k-1,c} p(x_{k-1}|c, Z^{k-1}) \quad (25)$$

where each element is termed a “track component” with index c and the total number of track components is C_{k-1} . In equation (25), $\xi_{k-1,c}$ denotes the relative probability that the track component c is true based on the measurement set Z^{k-1} ,

$$\xi_{k-1,c} \triangleq p(c|Z^{k-1}) \quad (26)$$

and

$$\sum_{c=1}^{C_{k-1}} \xi_{k-1,c} = 1. \quad (27)$$

The probability density function $p(x_{k-1}|c, Z^{k-1})$ is the target state pdf assuming that track component c is true and follows a Gaussian distribution:

$$p(x_{k-1}|c, Z^{k-1}) = \mathcal{N}(x_{k-1}; \hat{x}_{k-1|k-1}(c), P_{k-1|k-1}(c)) \quad (28)$$

where $\hat{x}_{k-1|k-1}(c)$ and $P_{k-1|k-1}(c)$ denotes the updated state estimate and error covariance of the track component c at time $k-1$ respectively.

3.2.1 Track Prediction

In equation (12), the predicted target trajectory state pdf $p(x_k|Z^{k-1})$ is calculated by

$$p(x_k|Z^{k-1}) = \int_{x_{k-1}} p(x_k|x_{k-1}) p(x_{k-1}|Z^{k-1}) dx_{k-1} \quad (29)$$

From the dynamic model of the target, we can observe that

$$p(x_k|x_{k-1}) = \mathcal{N}(x_k; Fx_{k-1}, Q_{k-1}) \quad (30)$$

Then, substituting (25) and (30) into (29)

$$\begin{aligned} p(x_k|Z^{k-1}) &= \int_{x_{k-1}} p(x_k|x_{k-1}) \\ &\quad \times \sum_{c=1}^{C_{k-1}} \xi_{k-1,c} p(x_{k-1}|c, Z^{k-1}) dx_{k-1} \end{aligned} \quad (31)$$

Interchanging the integral and summation yield

$$p(x_k|Z^{k-1}) = \sum_{c=1}^{C_{k-1}} \xi_{k-1,c} p(x_k|c, Z^{k-1}) \quad (32)$$

where

$$p(x_k|c, Z^{k-1}) = \mathcal{N}(x_k; \hat{x}_{k|k-1}(c), P_{k|k-1}(c)) \quad (33)$$

and each predicted track component comes from the standard Kalman filter prediction formulae

$$\hat{x}_{k|k-1}(c) = F\hat{x}_{k-1|k-1}(c) \quad (34)$$

$$P_{k|k-1}(c) = FP_{k-1|k-1}(c)F^T + Q_{k-1} \quad (35)$$

3.2.2 Track Update

Thus, both the measurement likelihood $p(z_k|x_k)$ and target prediction $p(x_k|Z^{k-1})$ are approximated by Gaussian mixtures, given by (24) and (32) respectively. Then, each measurement component updates each predicted track component, generating a new updated track component at time k .

The prior likelihood of measurement is given by

$$p(z_k|Z^{k-1}) = \int_{x_k} p(z_k|x_k) p(x_k|Z^{k-1}) dx_k \quad (36)$$

Applying (24) and (32), and interchanging the integral and summation, we can obtain

$$p(z_k|Z^{k-1}) = \sum_{i=1}^N \lambda_{k,i} p(z_{k,i}|Z^{k-1}) \quad (37)$$

where

$$\begin{aligned} p(z_{k,i}|Z^{k-1}) &= \sum_{c=1}^{C_{k-1}} \xi_{k-1,c} p(z_{k,i}|c, Z^{k-1}) \\ &= \sum_{c=1}^{C_{k-1}} \xi_{k-1,c} \mathcal{N}(z_{k,i}; \hat{z}_k(c), S_{k,i}(c)) \end{aligned} \quad (38)$$

and

$$\hat{z}_k(c) = H\hat{x}_{k|k-1}(c); \quad (39)$$

$$S_{k,i}(c) = HP_{k|k-1}(c)H^T + R_{k,i}. \quad (40)$$

$\hat{z}_k(c)$ and $S_{k,i}(c)$ are produced by the standard Kalman filter using the measurement components and predicted track components.

Substituting (24), (32) and (37) into (14), the *a posteriori* target state estimate pdf at time k can be calculated as

$$\begin{aligned} p(x_k|Z^k) &= \frac{\sum_{i=1}^N \lambda_{k,i} p(z_{k,i}|x_k) \sum_{c=1}^{C_{k-1}} \xi_{k-1,c} p(x_k|c, Z^{k-1})}{p(z_k|Z^{k-1})} \\ &= \sum_{c=1}^{C_{k-1}} \sum_{i=1}^N \frac{\xi_{k-1,c} \lambda_{k,i} p(z_{k,i}|x_k) p(x_k|c, Z^{k-1})}{p(z_k|Z^{k-1})} \\ &\quad \times \frac{p(z_{k,i}|c, Z^{k-1})}{p(z_{k,i}|c, Z^{k-1})} \\ &= \sum_{c=1}^{C_{k-1}} \sum_{i=1}^N \frac{\xi_{k-1,c} \lambda_{k,i} p(z_{k,i}|c, Z^{k-1})}{p(z_k|Z^{k-1})} \\ &\quad \times p(x_k|c, z_{k,i}, Z^{k-1}) \end{aligned} \quad (41)$$

which is reshaped into

$$p(x_k|Z^k) = \sum_{c^+=1}^{C_k} \xi_{k,c^+} p(x_k|c^+, z_k, Z^{k-1}) \quad (42)$$

where $c^+ = \{i, c\}$ denotes the new track component created by applying measurement component i to predicted track component c . Furthermore, the number of new track components at scan k increases to

$$C_k = C_{k-1} \cdot N. \quad (43)$$

The probability of the new track component is determined by the Bayes formula

$$\begin{aligned} \xi_{k,c^+} &\triangleq p(c, i|Z^k) \\ &= \frac{p(z_k|c, i, Z^{k-1})p(i|c, Z^{k-1})p(c|Z^{k-1})}{p(z_k|Z^{k-1})} \end{aligned} \quad (44)$$

Since the probability of the measurement component i does not depend on the previous measurements or the target state,

$$p(i|c, Z^{k-1}) = \lambda_{k,i} \quad (45)$$

Thus,

$$\xi_{k,c^+} = \frac{\lambda_{k,i} \xi_{k-1,c} p(z_k|c, i, Z^{k-1})}{p(z_k|Z^{k-1})} \quad (46)$$

where

$$p(z_k|c, i, Z^{k-1}) = \mathcal{N}(z_k; \hat{z}_k(c), S_{k,i}(c)) \quad (47)$$

and the prior measurement likelihood $p(z_k|Z^{k-1})$ can be calculated from (37). The relative probabilities ξ_{k,c^+} satisfy

$$\sum_{c^+=1}^{C_k} \xi_{k,c^+} = 1 \quad (48)$$

The state estimate of the new track component is given by

$$p(x_k|c^+, z_k, Z^{k-1}) = \mathcal{N}(x_k; \hat{x}_{k|k}(c^+), P_{k|k}(c^+)) \quad (49)$$

where $\hat{x}_{k|k}(c^+)$ and $P_{k|k}(c^+)$ are the mean value and the covariance matrix respectively, calculated by the standard Kalman filter update

$$\hat{x}_{k|k}(c^+) = \hat{x}_{k|k-1}(c) + K_k(c^+)(z_{k,i} - H\hat{x}_{k|k-1}(c)) \quad (50)$$

$$P_{k|k}(c^+) = (I - K_k(c^+)H)P_{k|k-1}(c) \quad (51)$$

with the Kalman gain

$$K_k(c^+) = P_{k|k-1}(c)H^T S_{k,i}^{-1}(c) \quad (52)$$

and $S_{k,i}(c)$ is given by (40).

3.2.3 Track Component Management

As described above, each measurement component is used to update each predicted track component and a new track component is generated. Obviously, the total number of track components grows exponentially over time. Thus, a practical implementation should be applied to control their number.

Existing available methods include track component pruning and component subtree removal (removing track components with low probability) (Blackman and Popoli, 1999), as well as track component merging. Track component merging merges track components that have similar states into one track component.

In this paper, the GMM-ITS implements the pruning and merging method proposed in (Singer et al., 1974), which proposes merging of all track components with the common measurement sequence.

3.2.4 Track Outputs

The track outputs usually consist of the mean and error covariance of the target estimate pdf, given by

$$\hat{x}_{k|k} = \sum_{c^+=1}^{C_k} \xi_{k,c^+} \hat{x}_{k|k}(c^+) \quad (53)$$

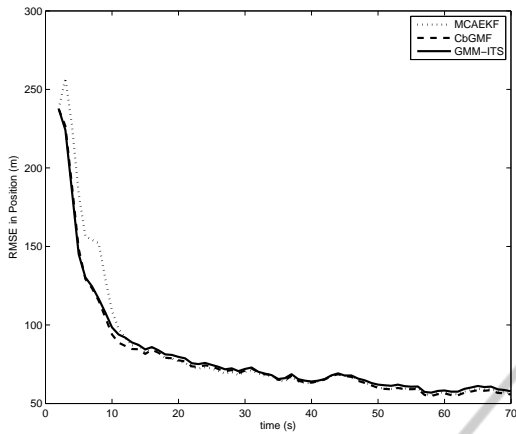
$$\begin{aligned} P_{k|k} &= \sum_{c^+=1}^{C_k} \xi_{k,c^+} (P_{k|k}(c^+) + \hat{x}_{k|k}(c^+) \hat{x}_{k|k}^T(c^+) \\ &\quad - \hat{x}_{k|k} \hat{x}_{k|k}^T) \end{aligned} \quad (54)$$

4 SIMULATION EXPERIMENTS

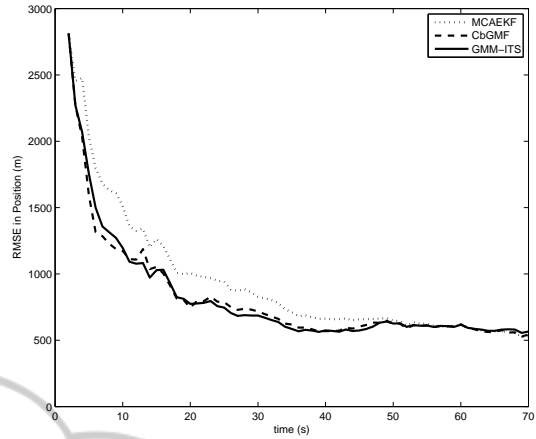
In this section, we evaluate the performance of the GMM-ITS in four scenarios where the target starts at different range from the sensor. We also compare it to the MCAEKF and the CbGMF.

In the simulation, the standard deviations of the measurements in range and azimuth are $\sigma_r = 0.2$ m and $\sigma_\theta = 10^{-3}$ rad, respectively. The sampling interval is $T = 1$ s, and the simulated time interval is 70 s. We choose the power spectral densities, $q_x = q_y = 10^{-3} \text{m}^2/\text{s}^3$. The target has the same initial velocity of [200, 300] m/s in different scenarios and the sensor always locates the origin.

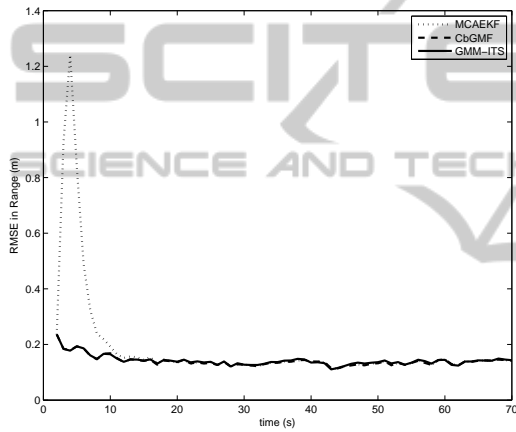
A two-point differencing method (Bar-Shalom et al., 2001) employing the unbiased measurement conversion (Longbin et al., 1998) from polar to Cartesian coordinates is used in the initialization of all filters. The results are obtained from 100 Monte Carlo runs.



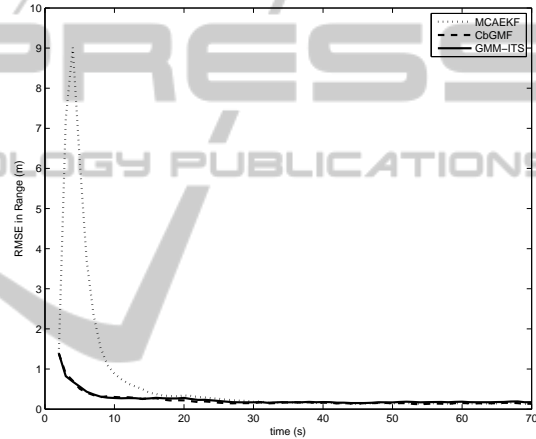
(a) RMSE in position



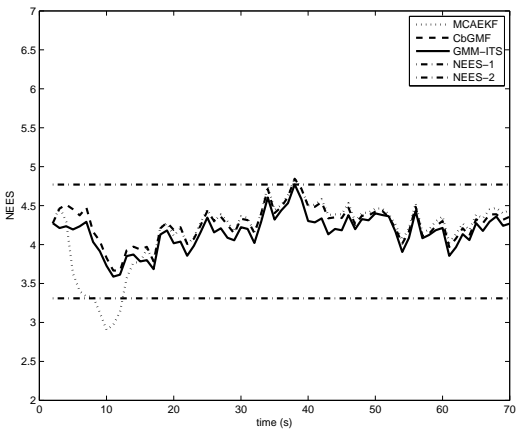
(a) RMSE in position



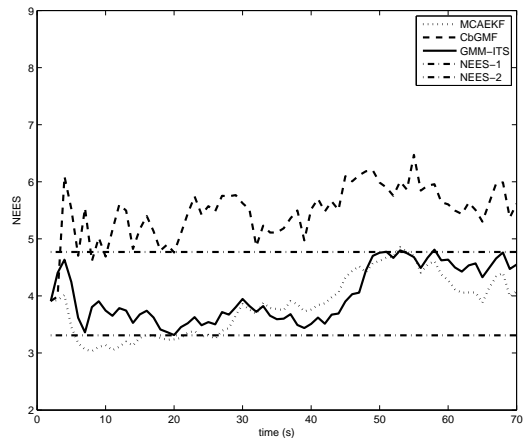
(b) RMSE in range



(b) RMSE in range



(c) NEES and 99% probability regions



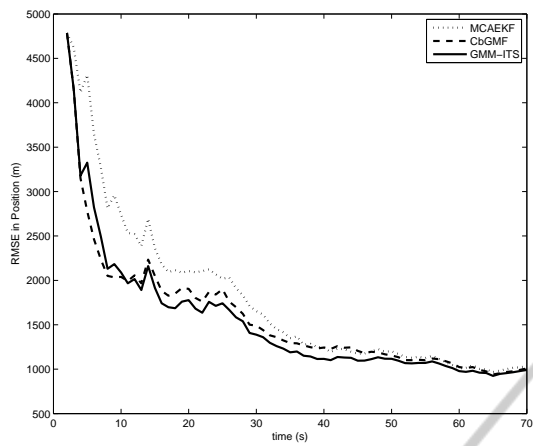
(c) NEES and 99% probability regions

Figure 3: Results from the medium range scenario.

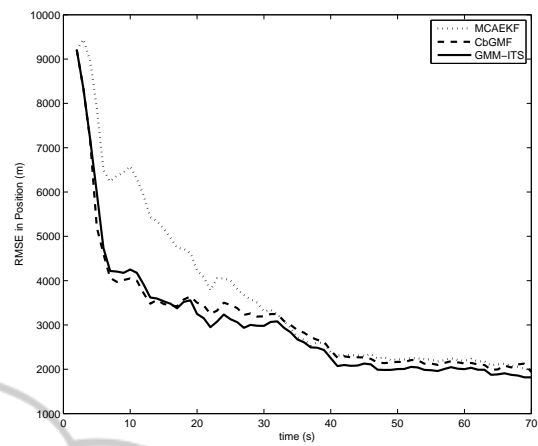
Figure 4: Results from the long range scenario.

We compare the accuracy of the filters using root mean square error (RMSE) (Bar-Shalom et al., 2001) in position and range. The normalized (state) estima-

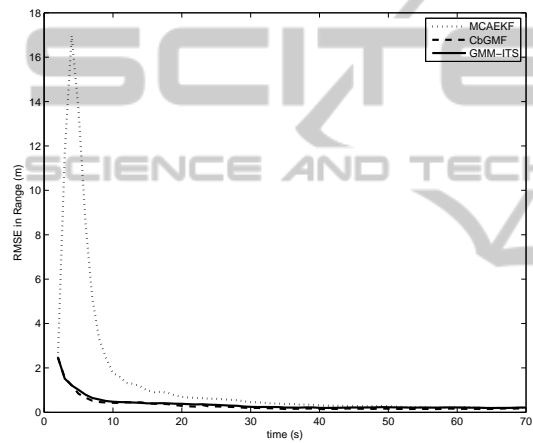
tion error squared (NEES) (Bar-Shalom et al., 2001) can be used to determine whether a filter is consistent. The results are presented in Figures 3-6.



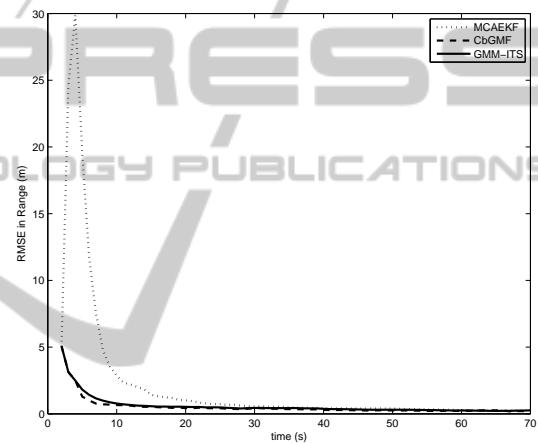
(a) RMSE in position



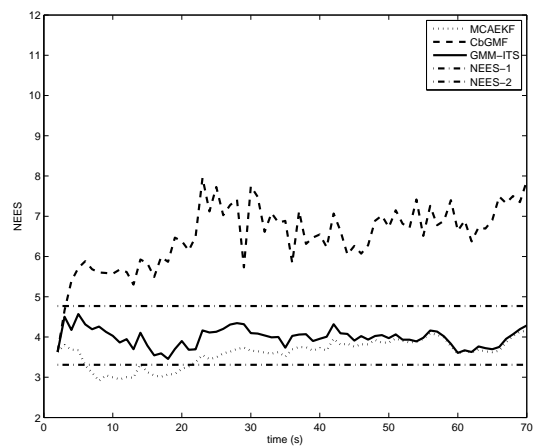
(a) RMSE in position



(b) RMSE in range

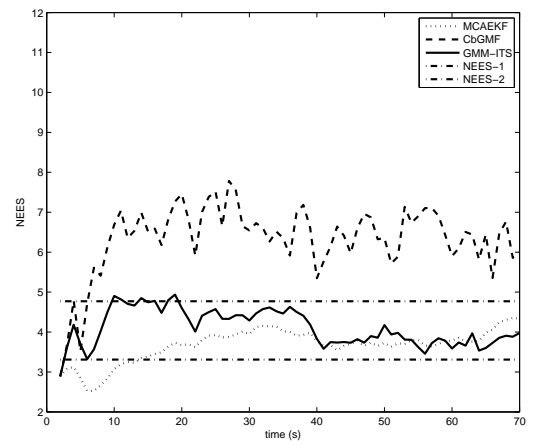


(b) RMSE in range



(c) NEES and 99% probability regions

Figure 5: Results from the very long range scenario



(c) NEES and 99% probability regions

Figure 6: Results from the extremely long range scenario.

In scenario 1, the target is initially located at [105, 250] km (the medium range). The GMM-ITS divides the measurement into $N = 6$ components and

chooses $\alpha = 3$ at each time k . Figures 3a, 3b and 3c shows the performance of the MCAEKF, the CbGMF and the GMM-ITS. These three filters have nearly the

same position accuracy (see Figure 3a) and good consistency (see Figure 3c). From Figure 3b, we can see that both the GMM-ITS and the CbGMF have significantly smaller range errors in the early states than the MCAEKF.

The target starts from [1050,2500] km (the long range) in scenario 2. In the GMM-ITS, the measurement likelihood is approximated by $N = 12$ components with $\alpha = 3$. In this scenario, as shown in Figures 4a, 4b and 4c, the GMM-ITS and the CbGMF have obviously improved accuracy in position and range over the MCAEKF and do not exhibit loss in range accuracy in the early stage of filtering. We can clearly see that the GMM-ITS and the MCAEKF are consistent in Figure 4c; however, in this case, the CbGMF has a small degradation in consistency (the NEES is around 5 instead of 4) (Tian and Bar-Shalom, 2014).

In scenario 3 and 4, the target starts much further away from [4500,2200] km (the very long range) and [8500,5500] km (the extremely long range), respectively. Obviously, the contact lens issue is much more of a problem than in scenario 1 and 2. In scenario 3, the parameters of the GMM-ITS are $N \equiv 24$ and $\alpha = 3.5$. In order to guarantee the consistency of the GMM-ITS, $N = 48$ and $\alpha = 4$ are chosen in scenario 4. Figures 5a and 6a show that the GMM-ITS performs better than the CbGMF and the MCAEKF in the position RMSE. Furthermore, as shown in Figure 5c and Figure 6c, the GMM-ITS and the MCAEKF are consistent, but the CbGMF is not.

5 CONCLUSIONS

For very long range target tracking, traditional filters such as the EKF and the UKF are ill-equipped to solve the contact lens problem. However, the MCAEKF maintains consistency by using a bigger standard deviation of the range measurement. As a result, the MCAEKF exhibits significant loss in range accuracy in the early stage of filtering. The CbGMF represents the distribution of the target state by a dynamic set of Gaussian mixtures and can avoid the problem the MCAEKF suffers. However, the CbGMF is consistent only in the small range scenario. In the GMM-ITS, both the measurement likelihood and the target state pdf are approximated by a set of Gaussian mixtures. As shown in the simulation experiments, the GMM-ITS is always consistent in different range scenarios and has small errors in position and range. To best of our knowledge, no other Gaussian mixture approach thus far guarantees sufficient consistency and tracking accuracy, which are crucial to filter performance.

ACKNOWLEDGEMENTS

This work was supported by Defense Acquisition Program Administration and Agency for Defense Development, Korea under the contract UD140081CD.

REFERENCES

- Bar-Shalom, Y., Li, X.-R., and Kirubarajan, T. (2001). *Estimation with Application to Tracking and Navigation*. John Wiley and Sons.
- Blackman, S. and Popoli, R. (1999). *Design and Analysis of Modern Tracking Systems*. Artech House.
- Julier, S. J. and Uhlmann, J. K. (2004). Unscented filtering and nonlinear estimation. *Proceedings of the IEEE*, 92(3):401–422.
- Longbin, M., Ziaoquan, S., Yiyu, Z., and Bar-Shalom, Y. (1998). Unbiased converted measurements for tracking. *IEEE Transactions on Aerospace and Electronic Systems*, 34(3):1023–1027.
- Mušicki, D. (2009). Bearings only single-sensor target tracking using gaussian mixtures. *Automatica*, 45(9):2088–2092.
- Mušicki, D. and Evans, R. (2006). Measurement gaussian sum mixture target tracking. In *9th International Conference on Information Fusion*, Florence, Italy.
- Ristic, B., Arulampalam, S., and Gordon, N. (2004). *Beyond the Kalman Filter*. Artech House.
- Singer, R. A., Sea, R., and Housewright, K. B. (1974). Derivation and evaluation of improved tracking filters for use in dense multi-target environments. *IEEE Transactions on Information Theory*, 20(4):423–432.
- Tian, X. and Bar-Shalom, Y. (2009). Coordinate conversion and tracking for very long range radars. *IEEE Transactions on Aerospace and Electronic Systems*, 45(3):1073–1088.
- Tian, X. and Bar-Shalom, Y. (2014). A consistency-based gaussian mixture filtering approach for the contact lens problem. *IEEE Transactions on Aerospace and Electronic Systems*, 50(3):1636–1646.